

COMPARISON OF EDGES DETECTED AT DIFFERENT POLARISATIONS IN MAESTRO DATA

Ronald G. Caves, Peter J. Harley and Shaun Quegan

Department of Applied and Computational Mathematics, University of Sheffield,
PO Box 597, Sheffield S10 2UN, England.

1. INTRODUCTION

Edge detection would appear to be a crucial tool for analysing multi-polarised, multi-frequency and multi-temporal Synthetic Aperture Radar (SAR) images. Edge structure provides a simple means for comparing different polarisations and frequencies, and for detecting changes over time. Due to the fact that edges and segments (homogeneous regions) are dual concepts, edge detection has an important role to play in identifying segments within which mean backscatter measurements for use in image classification can be made (*White 1991*).

As part of a general investigation into edge detection in SAR imagery, an initial investigation has been carried out into the detectability and nature of edges in multi-polarised and multi-frequency SAR images. The contrast ratio (CR) operator was used to detect edges. This operator has previously been shown to perform well at detecting edges in single-polarised and single-frequency SAR images (*Touzi et al. 1988; Caves et al. 1992*).

2. THE CONTRAST RATIO OPERATOR

At each point in an image the contrast ratio across a $n \times n$ window centred at that point is calculated by splitting the window into two equal sections, estimating the mean value of the pixels in each section and taking the ratio of these two mean values. Ratios are calculated for splits along the horizontal, vertical and two diagonal orientations. The largest ratio gives a measure of the contrast across the window. The larger the ratio, the greater the contrast, and the greater the likelihood that an edge exists at that point.

The contrast ratio image is thresholded to produce an edge map. So long as speckle is a stationary multiplicative noise process the false alarm rate in the edge map will be constant. Additionally, if it is assumed that speckle in an intensity image is uncorrelated and gamma distributed, the distribution of the contrast ratio can be determined and used to set a threshold for a desired probability of false alarm. The effects on the false alarm rate of known system induced correlation can be removed by sub-sampling within the processing window.

3. APPLICATION TO MAESTRO IMAGES

The CR operator was applied to C and P band MAESTRO single-look intensity images of Feltwell, UK. For each band the binary edge maps produced from two different polarisations were compared by overlaying them; the symbol

"o" is used to represent this binary operation (i.e. $\mathbf{HV} \circ \mathbf{VH} = \mathbf{HV} \times 2 + \mathbf{VH}$). This was done for all possible combinations of two different polarisations. Pixel values in the resulting 2-bit images indicated: 0 - no edge at either polarisation, 1 or 2 - an edge at one polarisation but not the other and 3 - an edge at both polarisations. The process was repeated with edge maps produced using different window sizes $n = 3, 5, \dots, 17$ and probabilities of false alarm $p = 10^{-3}, 10^{-4}, \dots, 10^{-6}$ (assuming exponential speckle). The correlation length in both range and azimuth was found to be two pixels; 2×2 sub-sampling was used within processing windows to remove its effect.

4. RESULTS

In each set of edge maps produced from the C band image using a particular window size and probability of false alarm, the greatest degree of similarity occurred between the edge maps of the cross-polarised terms (most values in $\mathbf{HV} \circ \mathbf{VH}$ were 0 or 3). A lesser degree of similarity occurred between the edge maps of the co-polarised terms. The most significant differences occurred between the edge maps of a co and a cross-polarised term. However due to the similarity of the edge maps of the cross-polarised terms, the differences occurring between the edge maps of a co-polarised term and the \mathbf{HV} term were similar to those occurring between the edge maps of the same co-polarised term and the \mathbf{VH} term.

These traits can be observed in figures 1 and 2 which show the results of edge detection using a 9×9 window with a probability of false alarm of $p = 10^{-4}$. Figure 1 shows the edge maps of the \mathbf{HH} , \mathbf{HV} and \mathbf{VV} terms and the result of combining the edge maps of all four polarisations. The edge maps of the single terms are all different from each other. Differences arise not just from edges being better defined in some polarisation than in others but also from features present in some polarisations being completely absent in others. The edge map of the \mathbf{HV} term contains significantly more detail than that of the \mathbf{HH} term which in turn contains slightly more detail more than that of the \mathbf{VV} term. The combined edge map is significantly more detailed than that of any single polarisation; each polarisation contributes something towards it.

Figure 2 shows histograms of combinations of edge maps of the (a) \mathbf{HH} and \mathbf{VV} , (b) \mathbf{HV} and \mathbf{VH} , (c) \mathbf{HH} and \mathbf{HV} , and (d) \mathbf{VV} and \mathbf{HV} terms using the "o" operator described above. The $\mathbf{HH} \circ \mathbf{VV}$ histogram shows that the percentage of edge pixels detected in the \mathbf{HH} term (i.e. those pixels with values 2 and 3) was greater than the percentage detected in the \mathbf{VV} term (pixels with values 1 and 3). The $\mathbf{HV} \circ \mathbf{VH}$ histogram shows that the small proportion of differences between the \mathbf{HV} and \mathbf{VH} terms is equally split between edges detected in the \mathbf{HV} term and not in the \mathbf{VH} term and edges detected in the \mathbf{VH} term and not in the \mathbf{HV} term. The $\mathbf{HH} \circ \mathbf{HV}$ and $\mathbf{VV} \circ \mathbf{HV}$ histograms show that the differences between co and cross-polarised terms is primarily due to a greater percentage of edges being detected in cross-polarised terms than in co-polarised terms. The total percentage of edges pixels in a given combination is indicated by subtracting the percentage of pixels with value 0 from 100. The greatest number of edges is detected by combining a co and a cross-polarised term and the least when the edge maps of the co-polarised terms are combined.

Apart from the \mathbf{HV} term, the P band image was much sharper than the C band image. This resulted in a much larger percentage of edges being detected. Once again the edge maps of cross-polarised terms were similar whilst edge maps of co-polarised terms were significantly different from those of cross-polarised

terms.

5. CONCLUSION

The CR operator has detected edge information useful for comparing differently polarised terms and for use in further processing. Significant differences exist between the edges detected in different polarisations. The most significant differences occurred between co and cross-polarised terms. The differences were small between cross-polarised terms, as reciprocity would predict. The images used were uncalibrated. However, assuming a linear system model, it can be shown that, to a good approximation calibration of this data involves only linear scalings of the intensity images (Quegan 1992). Such scalings would not affect the outcome of applying the CR operator. The fact that the images were not of comparable quality places more serious constraints on interpreting the results in terms of fundamental scattering properties of edges.

REFERENCES

- R. G. Caves, P. J. Harley and S. Quegan "Edge structure in ERS-1 and airborne SAR data," in *Proc. IGARSS'92* (Houston, USA), 1992.
- S. Quegan, "Cross-talk calibration of the MAESTRO data from the Reedham and Feltwell test-sites.", in *Proc. MAESTRO Final Workshop*, (Noordwijk, The Netherlands), 1992.
- R. Touzi, A. Lopes and P. Bousquet, "A statistical and geometrical edge detector for SAR images," *IEEE Trans. Geosci. Remote Sens.*, vol. 26, pp. 764-773, 1988.
- R. White, "Change detection in SAR imagery," *Int. J. Remote Sensing*, vol. 12, pp. 339-360, 1991.

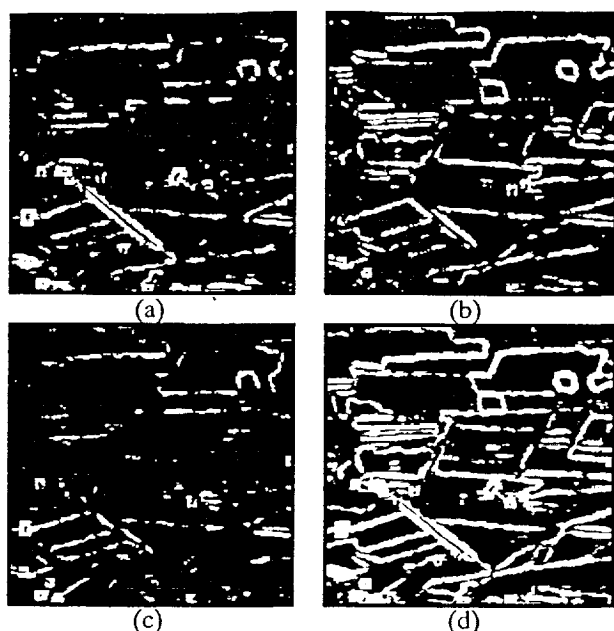


Figure 1. Edge maps of a MAESTRO C band image of an agricultural area produced using the contrast ratio operator with a 9×9 window and a probability of false alarm of 0.0001: (a) HH, (b) HV, (c) VV and (d) HH + HV + VH + HH.

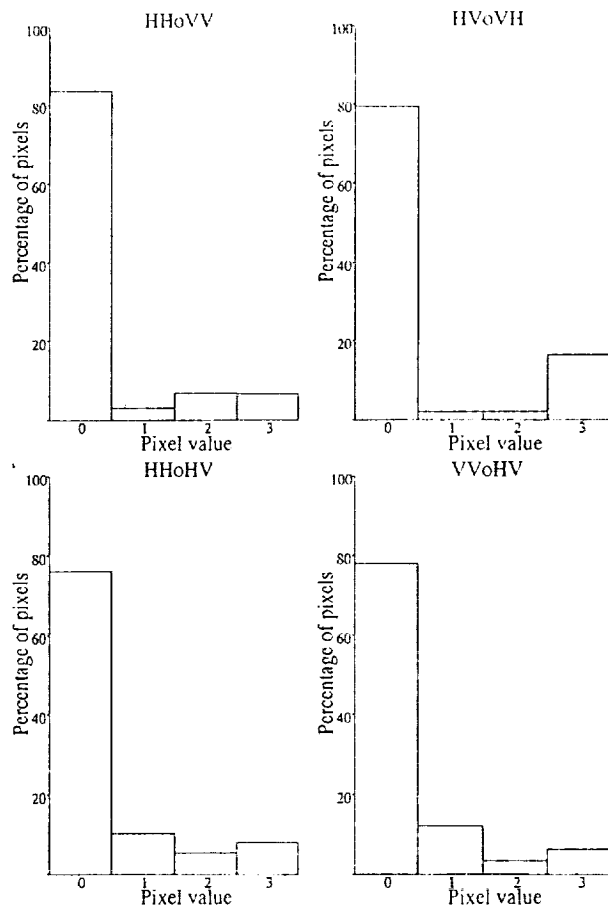


Figure 2. Histograms of combined edge maps.